Reductive N–N coupling of NO molecules on transition metal complexes leading to N_2O

Yasuhiro Arikawa[a,*] and Masayoshi Onishi[b]

[a] *Division of Chemistry and Materials Science, Graduate School of Engineering, Nagasaki University, Bunkyo-machi 1-14, Nagasaki 852-8521, Japan.*

[b] *Department of Applied Chemistry, Faculty of Engineering, Nagasaki University, Bunkyo-machi 1-14, Nagasaki 852-8521, Japan.*

Abstract

Nitric oxide reductase (NOR) type reactions ($2NO + 2e^- + 2H^+ \rightarrow N_2O + H_2O$) on transition metal complexes not involving NO disproportionation ($3NO \rightarrow N_2O + NO_2$) are reviewed. The former has little reported, although the latter is very common reaction. The formation of N_2O indicates that N–N coupling of two NO molecules is an essential step. A few examples of N–N coupling on transition metal complexes have been structurally characterized, including several examples of hyponitrite $(O\text{-}N{=}N\text{-}O)^{2-}$ complexes and only one diruthenium complex bearing neutral (O=N-N=O) binding mode. Protonation or heating their complexes led to elimination of N_2O. In the examination of the NOR-type reaction, only a few functional model complexes for the active site of the metalloenzyme have been developed. These complexes also showed NOR activity. Finally, an NO reduction cycle in the diruthenium system is described.

Keywords: Nitrogen monoxide; N–N coupling; Nitric oxide reductase (NOR); Nitrous oxide; Hyponitrite;

*Corresponding author. Tel./fax: +81 95 819 2673

E-mail address: arikawa@nagasaki-u.ac.jp

1. Introduction

The activation of relatively inert small molecules such as N_2 and CO_2 on transition metal complexes has been fascinating chemists [1]. While nitrogen monoxide (NO) is rather reactive compared with N_2 and CO_2, the controlled reactivity of NO on transition metal complexes has received considerably less attention. Since NO has an unpaired electron, oxidation to NO^+ or reduction to NO^- to generate electron paired species easily occurs, which complicates mechanistic understanding. Reactions involving NO regulation occur in biological systems [2], such as blood pressure control, neurotransmission, immune systems, etc., although NO has adverse effects on the environment [3]. Other exquisitely controlled reactivity of NO is shown in the metalloenzyme, nitric oxide reductase (NOR), which is involved in biological denitrification (a four-step process that reduces NO_3^- to N_2). NOR is a membrane-bound enzyme that catalyzes the $2e^-$ reduction of nitric oxide (NO) to nitrous oxide (N_2O) using two protons, i. e., $2NO + 2e^- + 2H^+ \rightarrow N_2O + H_2O$ [1,4]. In 2010, the crystal structure of NOR at 2.7 Å resolution was finally revealed [5]. The active site of NORs possesses a heme iron/non-heme iron (Fe_B) dinuclear center (Fig. 1), which is similar to that of the respiratory enzyme cytochrome *c* oxidase (CcO) [6], where Cu_B occupies the distal position instead of Fe_B in NOR. The mechanism of the NOR reaction remains a matter of debate [7]. However, it clearly involves intriguing N–N bond formation and N–O bond cleavage on transition metal complexes.

(Fig. 1 here)

The binding of NO to metal ions to afford metal-nitrosyl compounds can involve linear M-N-O geometry (NO^+) or bent M-N-O geometry ($NO^\bullet$ and NO^-). The geometry of M-N-O units can be predicted from the coordination number and the Enemark-Feltham electron counting formalism $\{MNO\}^n$, where *n* stands for the combined number of electrons on the metal d and π^*_{NO} orbitals (or *n* represents the number of d electrons on the metal when the NO is formally considered to be NO^+) [8]. This methodology has proved to be mostly successful to predict the coordination geometries of common metal-nitrosyl complexes, but several exceptions have been reported [9]. A number of comprehensive reviews and chapters about metal-NO complexes have appeared during the past several decades [10].

This review focuses on the NOR-type reaction (conversion of 2NO to N_2O and H_2O using two electrons and two protons) not involving NO disproportionation ($3NO \rightarrow N_2O + NO_2$) [1,4a,10]. Metal complex-mediated NO disproportionation is a very common reaction type. In either case, the N–N bond formation (N–N coupling) of two NO molecules on transition metals is a key step in the mechanism. However, only a few examples of N–N coupling on transition metals have been structurally characterized. In this connection two types of N–N coupling have

been determined, namely hyponitrite $(O\text{-}N{=}N\text{-}O)^{2-}$ formation and neutral (O=N-N=O) formation. There is only a single example of the latter. Initially, we describe these complexes and their ability to release N_2O. In addition, discussion about the NOR-type reaction using structural and functional models of the active site of NOR is reviewed. Finally, an NO reduction cycle utilizing the unprecedented N–N coupling (neutral (O=N-N=O) form) complex is described. Two recent reviews have also been written concerning hyponitrite interactions with transition-metal complexes and bioinspired inorganic chemistry involving NO reduction, respectively [11].

2. N–N coupling on transition metal complexes and elimination of N_2O

2.1. Hyponitrite $(O\text{-}N{=}N\text{-}O)^{2-}$ complexes and elimination of N_2O

Treatment of $Pt(PPh_3)_4$ with NO led to the reductive dimerization of NO to afford a *cis*-hyponitrite ligated Pt(II) complex $[Pt(ONNO)(PPh_3)_2]$ (**1a**) which was structurally characterized (Scheme 1) [12]. The *cis*-hyponitrite complexes $[L_nM(ONNO)]$ (M = Ni, Pt; L_n = PPh_3, PPh_2Me, dppe, and dppf) were also prepared by the reactions of $[L_nMCl_2]$ with diazeniumdiolate $RN_2O_2^-$ [13]. These complexes adopt a diamagnetic square planar geometry with an O-bonded planar chelating *cis*-hyponitrite ligand. These complexes were sensitive to acids, heat, light, and oxidation, producing N_2O and a transient terminal oxido complex $[L_nM{=}O]$ which was trapped by reactions with CO_2 or CS_2. In the thermolysis of [Ni(ONNO)(dppf)] (**1b**), the kinetics results indicate that the rate-limiting step is unimolecular involving release of N_2O.

(Scheme 1 here)

The reaction of a coordinatively unsaturated dinuclear complex $[Ru_2(CO)_4(\mu\text{-}H)(\mu\text{-}P^tBu_2)(\mu\text{-dppm})]$ with NO resulted in a *trans*-hyponitrite complex $[Ru_2(CO)_4(\mu\text{-}H)(\mu\text{-}P^tBu_2)(\mu\text{-dppm})(\mu\text{-ONNO})]$ (**2**) which was formed by reductive coupling of two NO molecules (Scheme 2) [14]. In the *trans*-$(ONNO)^{2-}$ ligand, one of two NO fragments bonds to the diruthenium core in the "side-on" manner, whereas the second one is not connected to the ruthenium. However, in the solid state the noncoordinating O atom exhibits a weak intramolecular bond to the carbon atom of a neighboring CO group. The $^{31}P\{^1H\}$ NMR spectrum of **2** shows three double doublet signals, and the ^1H NMR spectrum exhibits a multiplet hydride signal at δ = -12.30 ppm. The IR spectrum of **2** shows three bands for terminal carbonyl ligands and one characteristic band at 1742 cm^{-1}. The high nucleophilicity of the non-coordinated O atom was proved by O-protonation and -alkylation using HBF_4 and $[Me_3O]BF_4$, respectively, where the protonated **3a** and methylated **3b** complexes were confirmed by X-ray crystal structure analyses [15]. The IR spectra of **3a** and **3b** show only ν(CO) bands that are characteristic of terminal carbonyls, which differs from **2**. In their ^1H NMR spectra, singlet signals corresponding to the NO*H* and NO*Me* groups are observed at δ = 11.13 and 3.10 ppm, respectively. Deprotonation of **3b** afforded a neutral *trans*-hyponitrite derivative complex $[Ru_2(CO)_4(\mu\text{-}P^tBu_2)(\mu\text{-dppm})(\mu\text{-ONNOMe})]$ (**4**), which was also crystallographically characterized [16]. The ^1H NMR spectrum of **4** exhibits disappearance of the hydride signal. Although the *trans*-hyponitrite complex **2** was irradiated with UV in THF at room temperature to revert to the starting coordinatively unsaturated complex, thermolysis of the protonated complex **3a** afforded a hydroxido-bridged complex $[Ru_2(CO)_4(\mu\text{-}H)(\mu\text{-}OH)(\mu\text{-}P^tBu_2)(\mu\text{-dppm})]BF_4$, releasing N_2O. The bridging hydroxido group

is confirmed by a ν(OH) absorption band at 3567 cm^{-1} in the IR spectrum and a resonance signal at δ = -0.09 ppm in the ^1H NMR spectrum.

(Scheme 2 here)

A more complicated reaction between the cobalt carbonyl nitrosyl [$Co(CO)_3(NO)$] and excess NO gave a nitrito- and hyponitrito-bridged complex [($\{Co(NO)_2\}_2(\mu$-ONO))$_2(\mu$-ONNO)] (**5**) in low yields (Scheme 3) [17]. The IR spectrum of **5** shows two strong ν(NO) bands at 1850 and 1796 cm^{-1}, which are assignable to the terminal NO groups. The bridging hyponitrite group, which would be formed by reductive dimerization of NO, has a *trans* configuration, and its two NO fragments coordinate to the $\{Co(NO)_2\}_2(\mu$-ONO) unit in the "side-on" manner. The formation of the bridging nitrito ligands could arise from disproportionation of NO into NO_2 and N_2O. Pyrolysis of the hyponitrite complex **5** liberated N_2O along with NO, but not NO_2.

(Scheme 3 here)

On the other hand, the ammine cobalt complex $[Co(NH_3)_6]^{2+}$ was allowed to react with NO to afford various complexes, the formation of which is largely temperature dependent. Among them, a hyponitrito-bridged complex $[(NH_3)_5Co\{\mu$-N(O)NO$\}Co(NH_3)_5]^{4+}$ (**6**) was isolated and structurally characterized (Scheme 4) [18]. The two $Co(NH_3)_5$ units are bridged asymmetrically through a hyponitrite group, where one cobalt atom is bonded to an oxygen atom and the other to a nitrogen atom. The hyponitrite moiety is planar with a *cis* configuration. Acid treatments of the hyponitrite complex **6** in the absence of air produced N_2O and the aquapentaammine cobalt(III) complex.

(Scheme 4 here)

A hyponitrito-bridged iron porphyrin complex $[(OEP)Fe]_2(\mu$-ONNO) (**7**) (OEP= octaethylporphyrin) was prepared from the reaction of an oxido-bridged iron porphyrin complex $[(OEP)Fe]_2(\mu$-O) with hyponitrous acid (Scheme 5) [19]. The X-ray crystal structure reveals that the ONNO ligand is bound to each Fe via the κ^1-O binding mode and that the ONNO moiety is *trans*. The EPR spectral data of **7** (g = 5.74 and 2.03) as a CH_2Cl_2/toluene glass (77 K) is similar to that of two high-spin ferric hydroxido porphyrins. Protonation of the hyponitrite complex **7** at 0 ºC using HCl resulted in the formation of N_2O and [(OEP)FeCl]. The assumption that the protonation is initiated by H^+ attack on one of the O atoms of the hyponitrito bridge, followed by N-O bond cleavage to give N_2O, was proposed.

(Scheme 5 here)

The first example of the radical dianion of nitric oxide $(NO)^{2-}$ was discovered in an yttrium complex $\{[(Me_3Si)_2N]_2(THF)Y\}_2(\mu$-NO) (Scheme 6) [20]. This complex was allowed to react with another equivalent of NO to afford a diamagnetic *trans*-hyponitrite complex $\{[(Me_3Si)_2N]_2Y\}_4(\mu_3$-ONNO$)_2(THF)_2$ (**8**). The formation of the hyponitrite moiety can be

rationalized by the coupling of an NO radical with an $(NO)^{2-}$ radical: NO + $(NO)^{2-}$ -> $(ON=NO)^{2-}$. The $(ON=NO)^{2-}$ ligands chelate $Y\{N(SiMe_3)_2\}_2$ via N and O atoms, leading to four membered ring. The remaining O atom coordinates to $Y\{N(SiMe_3)_2\}_2(THF)$. The two dimers are bridged by the chelating O atoms, resulting in a tetranuclear complex. The reactivity of this complex has not been reported.

(Scheme 6 here)

2.2. N–N coupling (neutral (O=N-N=O) binding mode) complexes and elimination of N_2O

We found unique N–N coupling on dinuclear ruthenium complexes having Tp (= $HB(pyrazol\text{-}1\text{-}yl)_3$) ligands. These complexes were prepared from the reaction of $TpRuCl_2(NO)$ ($\{RuNO\}^6$) with pyrazoles in the presence of excess Et_3N (Scheme 7) [21]. The N-N coupling complexes $(TpRu)_2(\mu\text{-}Cl)(\mu\text{-}Rpz)\{\mu\text{-}N(=O)\text{-}N(=O)\}$ (**9**: $\{Ru_2(NO)_2\}^{14}$) consist of the bridging chlorido, pyrazolato, and N(=O)-N(=O) ligands. As can be seen from the Enemark-Feltham electron counting, $2e^-$ reduction occurred during the formation of **9**. This reductive formation is probably associated with the presence of the excess Et_3N, which is essential to the preparation. The X-ray result of **9a** shows that N–N distance is 1.861(3) Å (Fig. 2), which is much longer than that in the hyponitrite form, indicating NO dimer (vide infra) [22]. At low temperatures, NO molecules dimerize in the *cis* form with weak N–N bonding interaction (2.18 Å). DFT calculations of **9a** reproduce the molecular structure (N-N= 1.85325 Å), where the HOMO corresponds to N–N bonding (Fig. 2). Observation of such N–N coupling on transition metal sites not involving the hyponitrite form is unprecedented.

(Scheme 7 and Fig. 2 here)

Interestingly, reaction of the unusual N–N coupling complex **9** with an oxidizing agent ($AgBF_4$ or $[Cp_2Fe]BF_4$) giving $[\{TpRu(NO)\}_2(\mu\text{-}Cl)(\mu\text{-}pz)](BF_4)_2$ (**10**: $\{Ru_2(NO)_2\}^{12}$), led to N–N bond cleavage (Scheme 8). The IR spectrum of this product shows a characteristic ν(N≡O) band, and the structure was confirmed by the X-ray crystallographic analysis (Fig. 3). Bonding interaction between two NO nitrogen atoms is no longer observable as exemplified by an N···N separation of 3.006(8) Å. Reduction of the dinitrosyl complex **10** with Zn led to N–N bond formation, regenerating the N–N coupling complex **9**. The reversibility of this N–N bonding was supported by the cyclic voltammogram of the N–N coupling complex, which features a reversible two-electron redox process at 0.389 V ($E_{1/2}$ vs Ag/AgCl) (Fig. 4). Similar attempts to form an N–N bond between two nitrosyl ligands in a dinuclear iron complex have failed. In this case, warming of the dinitrosyl iron complex led to NO ligand dissociation (Scheme 9) [23].

(Scheme 8, Fig 3, Fig. 4, and Scheme 9 here)

Protonation of the N–N coupling complex **9** triggered elimination of N_2O (Scheme 10). Treatment of **9** with HBF_4 in CH_2Cl_2 gave an oxido-bridged dinuclear complex

$(TpRu)_2(\mu\text{-}Cl)(\mu\text{-}pz)(\mu\text{-}O)$ (**11**) (21% yield) and the oxidized complex **10** (43% yield), along with evolution of N_2O which was detected by gas-chromatography (25% yield based on **11**).

(Scheme 10 here)

2.3. Bond distances and angles and IR stretching frequencies for N_2O_2 frameworks of N–N coupling compounds

The N–N and N–O distances and O–N–N angles in the N_2O_2 framework are summarized in Table 1. In the hyponitrite complexes, the N–N (1.230 ~ 1.267 Å, average 1.255 Å) and N–O (1.307 ~ 1.400 Å, average 1.355 Å) bond distances are very similar to those of simple inorganic salts (*trans*-$Na_2(ONNO)$; N-N = 1.256(2) Å, N-O = 1.3622(11) Å) [24], leading to N–N double bond and N–O single bond, respectively. On the other hand, these distances of complex **9a** are obviously different from those of the hyponitrite complexes, but close to NO dimer.

(Table 1 here)

The IR spectra would give useful information of the appearance of the N_2O_2 moiety. The reported IR wavenumbers associated with the N_2O_2 stretching vibrations are shown in Table 2, involving those of the related complex $K_6[Co_2(CN)_{10}(N_2O_2)]$ [25], which is not X-ray crystallographically determined. The IR spectra of **1a** and **5** have been reported at the bands (**1a**, 1285, 1240, 1062 cm^{-1}; **5**, 1377, 1327, 1098, 828 cm^{-1}), but these are not clearly assigned [12b,17]. As can be seen in the IR spectra of two sodium hyponitrite [26], the *trans*- and *cis*-$N_2O_2^{2-}$ exhibit a single and three IR stretching vibrations, respectively, owing to their symmetry. Although the ν(NN) bands of the dinuclear ruthenium complexes (**2**–**4**) which have a *trans*-hyponitrite moiety are observed at 1425 ~ 1484 cm^{-1}, other hyponitrite complexes exhibit ν(NN) bands in the 1336 ~ 1399 cm^{-1} region. On the other hand, the IR spectra of the neutral N_2O_2 binding mode complexes **9**–**9b** show a characteristic ν(NO) band at ca. 1600 cm^{-1}. Assignment of the other ν(NO) band is probably hindered by overlapping with the bands associated with pyrazole.

(Table 2 here)

3. NOR-type reaction using functional model complexes

In the examination of the NOR-type reaction, use of the enzymes makes it difficult to elucidate the NO reduction mechanism. Lu et al. have reported excellent engineered metalloproteins to mimic the structure and function of the NOR active site, where three histidines (His) and one or two glutamates (Glu) were introduced in sperm whale myoglobin [27]. Although three His and one Glu residues bind iron, mimicking the Fe_B site in NOR, introducing the second Glu to the second coordination sphere of the Fe_B site through a hydrogen bonding network resulted in ~100% increase in NOR activity. Also, the synthetic model complexes that mimic the active site of NOR can help mechanistic understanding. However, only a few synthetic model complexes have been developed.

3.1. Heme Fe/tripyridyl Fe dinuclear system

Karlin et al. have designed model ligands that contain a tetradentate tris(2-pyridylmethyl)amine chelate tethered to a tetraarylporphyrin [28–31]. A heme/non-heme diiron(II) complex $[(^5L)Fe^{II}\cdots Fe^{II}\text{-}Cl]^+$ (**12**) was prepared and allowed to react with NO at low complex concentrations (below 10 μM) to give an oxido bridged complex $[(^5L)Fe^{III}\text{-}O\text{-}Fe^{III}\text{-}Cl]^+$ (Scheme 11) [28]. This indicates that each iron contributes one electron and the two NO ligands couple to give N_2O (reductive dimerization) leaving the O-atom in the oxido bridged complex. However, N_2O was not detected probably because of low concentrations. At high concentrations, both N_2O and NO_2 were detected. Therefore Karlin et al. have proposed that N_2O is formed via reductive dimerization and NO_2 is produced by the reaction of the resulting oxido bridged complex $[(^5L)Fe^{III}\text{-}O\text{-}Fe^{III}\text{-}Cl]^+$ with NO. With the related complex $[(^6L)Fe^{II}\cdots Fe^{II}\text{-}Cl]^+$, reaction with NO gave a bis-nitrosyl adduct $[(^6L)Fe^{II}(NO)Fe^{II}(NO)\text{-}Cl]^+$ (**13**) [30]. However, complex **13** is very stable and NO-reductive coupling was not observed upon the addition of proton sources or excess base. Instead, the addition of excess base resulted in ligand-promoted NO dissociation to give $[(^6L)Fe^{II}\cdots Fe^{II}\text{-}Cl]^+$.

(Scheme 11 here)

3.2. Heme Fe/tripyridyl Cu dinuclear system

Interestingly, the NOR activity (NO reduction to N_2O) has been found in a heme/copper dinuclear reaction system. This resembles heme-copper oxidases, including cytochrome *c* oxidases (CcO), that are evolutionarily related to NOR. A dinitrosyl complex $(^6L)Fe(NO)_2$ (**14**) was synthesized at low temperatures and allowed to react with a copper source, $[Cu^I(MeCN)_4]B(C_6F_5)_4$, and 2 equiv acid ($H(OEt_2)_2[B(C_6F_5)_4]$) to afford N_2O in very good yield and $[(^6L)Fe^{III}\cdots Cu^{II}(D)]^{3+}$ (D = MeCN or H_2O) (Scheme 12) [31]. In control experiments,

the dinitrosyl complex **14** was protonated at -80 ºC and then warmed to room temperature to afford a mono nitrosyl complex (^{6}L)Fe(NO), releasing NO. On the other hand, absence of protons led to N_2O and a heme-nitrosyl···Cu-nitrite complex $[(^6L)Fe(NO)\cdots Cu^{II}(NO_2^-)]^+$, indicating a copper complex mediated disproportionation reaction. Thus, a stoichiometric functional model system for heme/nonheme diiron NOR has been demonstrated, i. e., $[(^6L)Fe^{II}\cdots Cu^{I}]^+ + 2NO + 2H^+ \rightarrow [(^6L)Fe^{III}\cdots Cu^{II}]^+ + N_2O + H_2O$.

(Scheme 12 here)

Moreover, a 1:1 mixture of a heme $(F_8)Fe$ (F_8 = tetrakis(2,6-difluorophenyl)porphyrinate(2-)) and a copper complex $[(tmpa)Cu^{I}(MeCN)]^+$ (tmpa = tris(2-pyridylmethyl)amine) components has also facilitated NO reduction to N_2O. A dinitrosyl complex $(F_8)Fe(NO)_2$ (**15**) was allowed to react with $[(tmpa)Cu^{I}(MeCN)]^+$ and 2 equiv of acid ($H(OEt_2)_2[B(C_6F_5)_4]$) to afford $[(F_8)Fe^{III}]^+$, $[(tmpa)Cu^{II}(solvent)]^{2+}$, and N_2O (Scheme 13) [32], corresponding to the stoichiometric NO reductive coupling reaction: $2NO + Fe^{II} + Cu^{I} + 2H^+ \rightarrow N_2O + Fe^{III} + Cu^{II} + H_2O$. Control experiments showed that both iron and copper centers are required for the observed NOR-type chemistry and that, if acid is not present, half of the NO is trapped as a $(F_8)Fe(NO)$ complex, while the remaining NO undergoes copper complex promoted disproportionation chemistry. Heme–Fe^{II}, Cu^{I}, and acid are all required to trigger the NOR-type reaction. The protonated hyponitrite ($HONNO^-$) dinuclear intermediate, where N atoms bind to both the metal ions, has been suggested. This protonated hyponitrite intermediate (*trans*-mechanism) has been also supported by biophysical studies and DFT calculations [7].

(Scheme 13 here)

3.3. Heme Fe/trisimidazole Fe dinuclear system

Collman et al. have reported biomimetic ligands featuring a porphyrin with three imidazole pickets at the distal site and an imidazole ligand at the proximal site. Both the distal and proximal ligands are covalently attached to the porphyrin [33,34]. Collman et al. prepared the synthetic model complex LFe^{II}/Fe^{II} (**16**), which was allowed to react with two equivalents of NO to give one equivalent of N_2O and a bis-ferric product LFe^{III}-NO/Fe^{III}-OH (Scheme 14) [34]. During the NO reduction, the proximal imidazole remains coordinated to the heme iron, which enhances the radical character of the heme nitrosyl. This should be advantageous for the N–N coupling step. On the other hand, the reaction of the mixed-valence form LFe^{III}/Fe^{II} with NO gave a mixture of LFe^{III}-NO/Fe^{II}-NO and LFe^{II}-NO/Fe^{III} without NO reduction. The spectroscopic data of the NO reduction reaction indicates that the first NO binds to Fe_B forming a high-spin Fe_B–NO species (A), followed by another NO binding to heme Fe^{II}. This results in the formation of an LFe^{II}–NO/Fe–NO species (B) which then forms N_2O and the bis-ferric

product LFe^{III}-NO/Fe^{III}-OH. Interestingly, these data also indicate that in the bis-nitrosyl intermediate B the two nitrosyls are close enough to either spin-dipole couple or directly interact.

(Scheme 14 here)

4. NO reduction cycle (Ru dinuclear system supported by Tp ligands)

Our ruthenium system has achieved an NO reduction cycle. The oxido-bridged complex **11**, which was produced by proton-induced elimination of N_2O in **9**, was allowed to react with 1 equiv of HBF_4 in diethyl ether to give a hydroxido-bridged dinuclear ruthenium complex $[(TpRu)_2(\mu\text{-}Cl)(\mu\text{-}OH)(\mu\text{-}pz)]BF_4$ (**17**) (Scheme 15) [21b]. The ^1H NMR spectrum of **17** indicates paramagnetism, although the NMR spectrum of **11** shows diamagnetism probably owing to strong antiferromagnetic spin exchange coupling via a superexchange mechanism [35]. Protonation of the oxido bridge in **11** weakens the orbital overlap between the Ru dπ and oxygen pπ orbitals, resulting decrease of the antiferromagnetic coupling. Finally, the structure of **17** was determined by single-crystal X-ray diffraction. Protonation on the bridged oxido ligand was confirmed by the Ru-O distance (2.0038(19) Å), which is longer than that of 4-bromopyrazolato- and oxido-bridged derivative of **11** (1.898(4), 1.904(3) Å) [21a]. Additional protonation of **17** should give an aqua-bridged dinuclear ruthenium $[(TpRu)_2(\mu\text{-}OH_2)(\mu\text{-}Cl)(\mu\text{-}pz)](BF_4)_2$ (**18**). Thus in the ^1H NMR spectrum, when HBF_4 was added to an acetone-d_6 solution of **17**, one set of paramagnetic signals appeared, which can be assigned to **18**. Isolation of **18** failed, probably owing to easy deprotonation. However, its formation in the reaction mixture was detected by FAB-MS spectroscopy. Thus, after treatment of **17** with HBF_4 for 15h, the reaction mixture was exposed to NO to give the dinitrosyl complex **10** in 53% yield. Reduction of the dinitrosyl complex **10** induced N–N coupling of the two NO ligands, affording the complex **9** (vide supra). These successes led to completion of an NO reduction cycle on the dinuclear ruthenium complex (Scheme 16).

(Scheme 15 and Scheme 16 here)

5. Summary

The NOR-type reactions ($2NO + 2e^- + 2H^+ \rightarrow N_2O + H_2O$) are reviewed. In connection with this, several structurally characterized hyponitrite $(O\text{-}N{=}N\text{-}O)^{2-}$ complexes and one diruthenium complex bearing an unusual neutral (O=N-N=O) ligand are reported. All of these complexes, except for the yttrium complex **8** where its reactivity is not reported, released N_2O by protonation and heat. Also, a few functional model complexes for the active site of the metalloenzyme (nitric oxide reductase) showed NOR activity. Finally, the NO reduction cycle using the unprecedented N–N coupling complex **9** is presented.

Acknowledgements

This work was supported by a Grant-in-Aid for Young Scientists (A) (No. 22685008) from the Japan Society for the Promotion of Science and by a Grant-in-Aid for Scientific Research from Nagasaki University.

References

[1] W.B. Tolman, Activation of Small Molecules, Wiley-VCH, Weinheim, 2006.

[2] (a) J. Lancaster, Jr., Nitric Oxide: Principles and Actions, Academic Press, San Diego, 1996;

(b) L.J. Ignarro, Nitric Oxide: Biology and Pathobiology, Academic Press, San Diego, 2000.

[3] J. Lelieveld, P.J. Crutzen, Science, 264 (1994) 1759.

[4] (a) I.M. Wasser, S. de Vries, P. Moënne-Loccoz, I. Schröder, K.D. Karlin, Chem. Rev., 102 (2002) 1201;

(b) P. Tavares, A.S. Pereira, J.J.G. Moura, I. Moura, J. Inorg. Biochem., 100 (2006) 2087;

(c) W.G. Zumft, J. Inorg. Biochem., 99 (2005) 194;

(d) E. Pinakoulaki, S. Gemeinhardt, M. Saraste, C. Varotsis, J. Biol. Chem., 277 (2002) 23407;

(e) J. Hendriks, A. Warne, U. Gohlke, T. Haltia, C. Ludovici, M. Lübben, M. Saraste, Biochemistry, 37 (1998) 13102;

(f) P. Girsch, S. de Vries, Biochim. Biophys. Acta, 1318 (1997) 202;

(g) B.A. Averill, Chem. Rev., 96 (1996) 2951;

[5] T. Hino, Y. Matsumoto, S. Nagano, H. Sugimoto, Y. Fukumori, T. Murata, S. Iwata, Y. Shiro, Science, 330 (2010) 1666.

[6] (a) G.T. Babcock, M. Wikström, Nature, 356 (1992) 301;

(b) S. Ferguson-Miller, G.T. Babcock, Chem. Rev., 96 (1996) 2889;

(c) B. Ludwig, E. Bender, S. Arnold, M. Hüttemann, I. Lee, B. Kadenbach, ChemBioChem., 2 (2001) 392;

(d) J.P. Collman, R.A. Decréau, Chem. Commun. (2008) 5065.

[7] Three putative reaction mechanisms (*trans*-mechanism, *cis*-Fe_B mechanism, and *cis*-heme b_3 mechanism) have been proposed;

(a) P. Moënne-Loccoz, Nat. Prod. Rep., 24 (2007) 610;

(b) E. Pinakoulaki, C. Varotsis, J. Inorg. Biochem., 102 (2008) 1277;

(c) C. Varotsis, T. Ohta, T. Kitagawa, T. Soulimane, E. Pinakoulaki, Angew. Chem., Int. Ed., 46 (2007) 2210;

(d) T. Hayashi, I.-J. Lin, Y. Chen, J.A. Fee, P. Moënne-Loccoz, J. Am. Chem. Soc., 129 (2007) 14952;

(e) L.M. Blomberg, M.R.A. Blomberg, P.E.M. Siegbahn, Biochim. Biophys. Acta, 1757 (2006) 31;

(f) L.M. Blomberg, M.R.A. Blomberg and P.E.M. Siegbahn, Biochim. Biophys. Acta, 1757 (2006) 240;

(g) T. Ohta, T. Kitagawa, C. Varotsis, Inorg. Chem., 45 (2006) 3187;
(h) X. Zhao, N. Yeung, B.S. Russell, D.K. Garner, Y. Lu, J. Am. Chem. Soc., 128 (2006) 6766;
(i) E. Pinakoulaki, T. Ohta, T. Soulimane, T. Kitagawa, C. Varotsis, J. Am. Chem. Soc., 127 (2005) 15161;
(j) H. Kumita, K. Matsuura, T. Hino, S. Takahashi, H. Hori, Y. Fukumori, I. Morishima, Y. Shiro, J. Biol. Chem., 279 (2004) 55247;
(k) E. Pinakoulaki, S. Stavrakis, A. Urbani, C. Varotsis, J. Am. Chem. Soc., 124 (2002) 9378;
(l) S. Stavrakis, E. Pinakoulaki, A. Urbani, C. Varotsis, J. Phys. Chem. B, 106 (2002) 12860;
(m) P. Moënne-Loccoz, O.-M.H. Richter, H.-W. Huang, I.M. Wasser, R.A. Ghiladi, K.D. Karlin, S. de Vries, J. Am. Chem. Soc., 122 (2000) 9344;
(n) P. Moënne-Loccoz, S. de Vries, J. Am. Chem. Soc., 120 (1998) 5147;
(o) C.S. Butler, H.E. Seward, C. Greenwood, A.J. Thomson, Biochemistry, 36 (1997) 16259;
(p) R.W. Ye, B.A. Averill, J.M. Tiedje, Appl. Environ. Microbiol., 60 (1994) 1053.

[8] (a) J.H. Enemark, R.D. Feltham, Coord. Chem. Rev., 13 (1974) 339;
(b) R.D. Feltham, J.H. Enemark, Top. Stereochem., 12 (1981) 155;
(c) B.L. Westcott, J.H. Enemark, in: E.I. Solomon, A.B.P. Lever (Eds.), Inorganic Electronic Structure and Spectroscopy, Vol. II, Wiley, New York, 1999, pp. 403–450.

[9] Richter-Addo, G.B., R.A. Wheeler, C.A. Hixson, L. Chen, M.A. Khan, M.K. Ellison, C.E. Schulz, W.R. Scheidt, J. Am. Chem. Soc., 123 (2001) 6314.

[10] (a) G.B. Richter-Addo, P. Legzdins, J. Burstyn, Chem. Rev., 102 (2002) 857;
(b) T.W. Hayton, P. Legzdins, W.B. Sharp, Chem. Rev., 102 (2002) 935;
(c) P.C. Ford, I.M. Lorkovic, Chem. Rev., 102 (2002) 993;
(d) G.B. Richter-Addo, P. Legzdins, Metal Nitrosyls, Oxford University Press, New York, 1992;
(e) J.A. McCleverty, Chem. Rev., 104 (2004) 403;
(f) F. Roncaroli, M. Videla, L.D. Slep, J.A. Olabe, Coord. Chem. Rev., 251 (2007) 1903.

[11] (a) Xu, N., J. Yi, G.B. Richter-Addo, Inorg. Chem. 49 (2010) 6253;
(b) Schopfer, M.P., J. Wang, K.D. Karlin, Inorg. Chem. 49 (2010) 6267.

[12] (a) S. Bhaduri, B.F.G. Johnson, A. Pickard, P.R. Raithby, G.M. Sheldrick, C.I. Zuccaro, J. Chem. Soc. Chem. Commun. (1977) 354.
(b) Cenini, S., R. Ugo, G. LaMonica, S.D. Robinson, Inorg. Chim. Acta. 6 (1972) 182.

[13] (a) N. Arulsamy, D.S. Bohle, J.A. Imonige, R.C. Moore, Polyhedron, 26 (2007) 4737;

(b) N. Arulsamy, D.S. Bohle, J.A. Imonige, S. Levine, Angew. Chem., Int. Ed., 41 (2002) 2371.

[14] H.-C. Böttcher, M. Graf, K. Mereiter, K. Kirchner, Organometallics, 23 (2004) 1269.

[15] H.-C. Böttcher, C. Wagner, K. Kirchner, Inorg. Chem., 43 (2004) 6294.

[16] H.-C. Böttcher, P. Mayer, Inorg. Chim. Acta., 363 (2010) 799.

[17] R. Bau, I.H. Sabherwal, A.B. Burg, J. Am. Chem. Soc., 93 (1971) 4926.

[18] (a) P. Gans, J. Chem. Soc. (A), (1967) 943;
(b) B.F. Hoskins, F.D. Whillans, Chem. Comm. (1969) 69;
(c) B.F. Hoskins, F.D. Whillans, J. Chem. Soc. Dalton (1973) 607;
(d) M.E. Chacón Villalba, A. Navaza, J.A. Güida, E.L. Varetti, P.J. Aymonino, Inorg. Chim. Acta., 359 (2006) 707.

[19] N. Xu, A.L.O. Campbell, D.R. Powell, J. Khandogin, G.B. Richter-Addo, J. Am. Chem. Soc., 131 (2009) 2460.

[20] W.J. Evans, M. Fang, J.E. Bates, F. Furche, J.W. Ziller, M.D. Kiesz, J.I. Zink, Nature Chemistry, 2 (2010) 644.

[21] (a) Y. Arikawa, T. Asayama, Y. Moriguchi, S. Agari, M. Onishi, J. Am. Chem. Soc., 129 (2007) 14160;
(b) Y. Arikawa, N. Matsumoto, T. Asayama, K. Umakoshi, M. Onishi, Dalton Trans., 40 (2011) 2148.

[22] (a) W.N. Lipscomb, J. Chem. Phys., 54 (1971) 3659;
(b) W.N. Lipscomb, F.E. Wang, Acta Cryst., 14 (1961) 1100;
(c) W.J. Dulmage, E.A. Meyers, W.N. Lipscomb, Acta Cryst., 6 (1953) 760.
(d) Dinerman, C.E., G.E. Ewing, J. Chem. Phys. 53 (1970) 626–631.

[23] A.L. Feig, M.T. Bautista, S.J. Lippard, Inorg. Chem., 35 (1996) 6892.

[24] N. Arulsamy, D.S. Bohle, J.A. Imonigie, E.S. Sagan, Inorg. Chem., 38 (1999) 2716.

[25] Jeżowska-Trzebiatowska, B., J. Hanuza, M. Ostern, J. Ziółkowski, Inorg. Chim. Acta. 6 (1972) 141.

[26] (a) Goubeau, J., K. Laitenberger, Z. Anorg. Allg. Chem. 320 (1963) 78;
(b) Kuhn, L., E.R. Lippincott, J. Am. Chem. Soc. 78 (1956) 1820.

[27] (a) Yeung, N., Y.-W. Lin, Y.-G. Gao, X. Zhao, B.S. Russell, L. Lei, K.D. Miner, H. Robinson, Y. Lu, Nature 462 (2009) 1079;
(b) Lin, Y.-W., N. Yeung, Y.-G. Gao, K.D. Miner, S. Tian, H. Robinson, Y. Lu, Proc. Nat. Acad. Sci. USA 107 (2010) 8581;
(c) Hayashi, T., K.D. Miner, N. Yeung, Y.-W. Lin, Y. Lu, P. Moënne-Loccoz, Biochemistry 50 (2011) 5939.

[28] T.D. Ju, A.S. Woods, R.J. Cotter, P. Moënne-Loccoz, K.D. Karlin, Inorg. Chim. Acta, 297

(2000) 362.

[29] I.M. Wasser, C.F. Martens, C.N. Verani, E. Rentschler, H.-W. Huang, P. Moënne-Loccoz, L.N. Zakharov, A.L. Rheingold, K.D. Karlin, Inorg. Chem., 43 (2004) 651.

[30] I.M. Wasser, H.-W. Huang, P. Moënne-Loccoz, K.D. Karlin, J. Am. Chem. Soc., 127 (2005) 3310.

[31] J. Wang, M.P. Schopfer, A.A.N. Sarjeant, K.D. Karlin, J. Am. Chem. Soc., 131 (2009) 450.

[32] J. Wang, M.P. Schopfer, S.C. Puiu, A.A.N. Sarjeant, K.D. Karlin, Inorg. Chem., 49 (2010) 1404.

[33] (a) J.P. Collman, Y.-L. Yan, J. Lei, P.H. Dinolfo, Inorg. Chem., 45 (2006) 7581;
(b) J.P. Collman, A. Dey, R.A. Decréau, Y. Yang, A. Hosseini, E.I. Solomon, T.A. Eberspacher, Proc. Nat. Acad. Sci. USA, 105 (2008) 9892.

[34] (a) J.P. Collman, Y. Yang, A. Dey, R.A. Decréau, S. Ghosh, T. Ohta, E.I. Solomon, Proc. Nat. Acad. Sci. USA, 105 (2008) 15660;
(b) J.P. Collman, A. Dey, Y. Yang, R.A. Decréau, T. Ohta, E.I. Solomon, J. Am. Chem. Soc., 130 (2008) 16498.

[35] (a) R. Hotzelmann, K. Wieghardt, U. Flörke, H.-J. Haupt, D.C. Weatherburn, J. Bonvoisin, G. Blondin, J.-J. Girerd, J. Am. Chem. Soc., 114 (1992) 1681;
(b) R. Hotzelmann, K. Wieghardt, J. Ensling, H. Romstedt, P. Gütlich, E. Bill, U. Flörke, H.-J. Haupt, J. Am. Chem. Soc., 114 (1992) 9470.

[Captions]

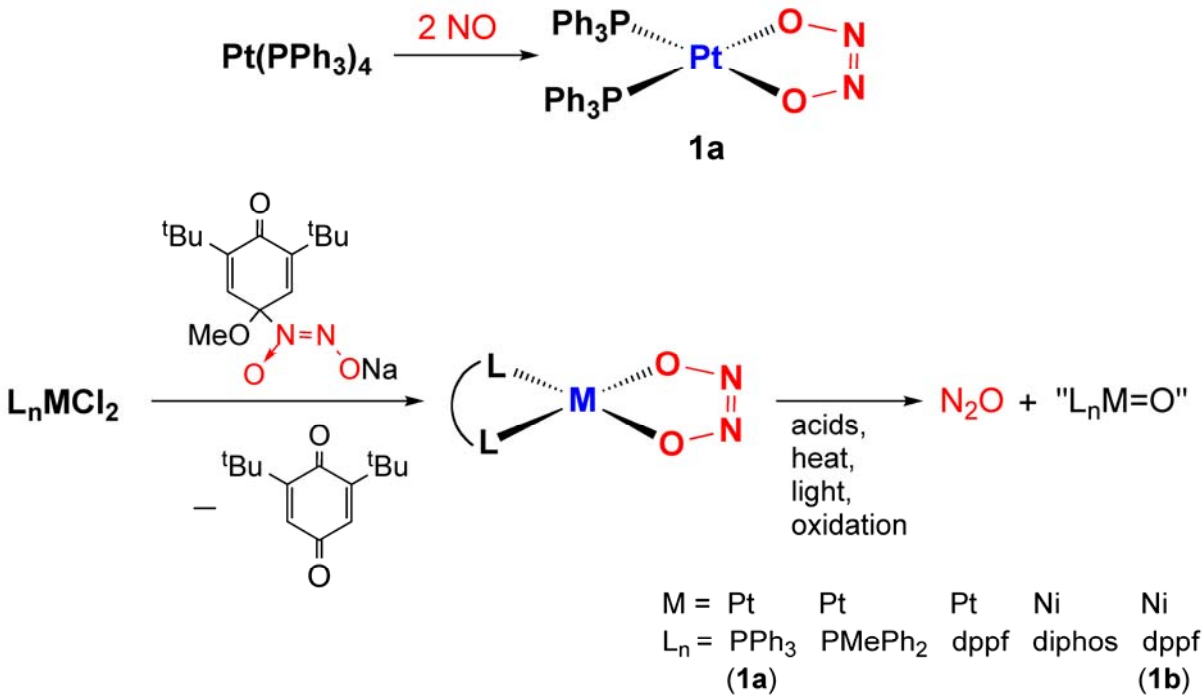

Scheme 1. Syntheses of group 10 hyponitrite complexes **1** and elimination of N_2O.

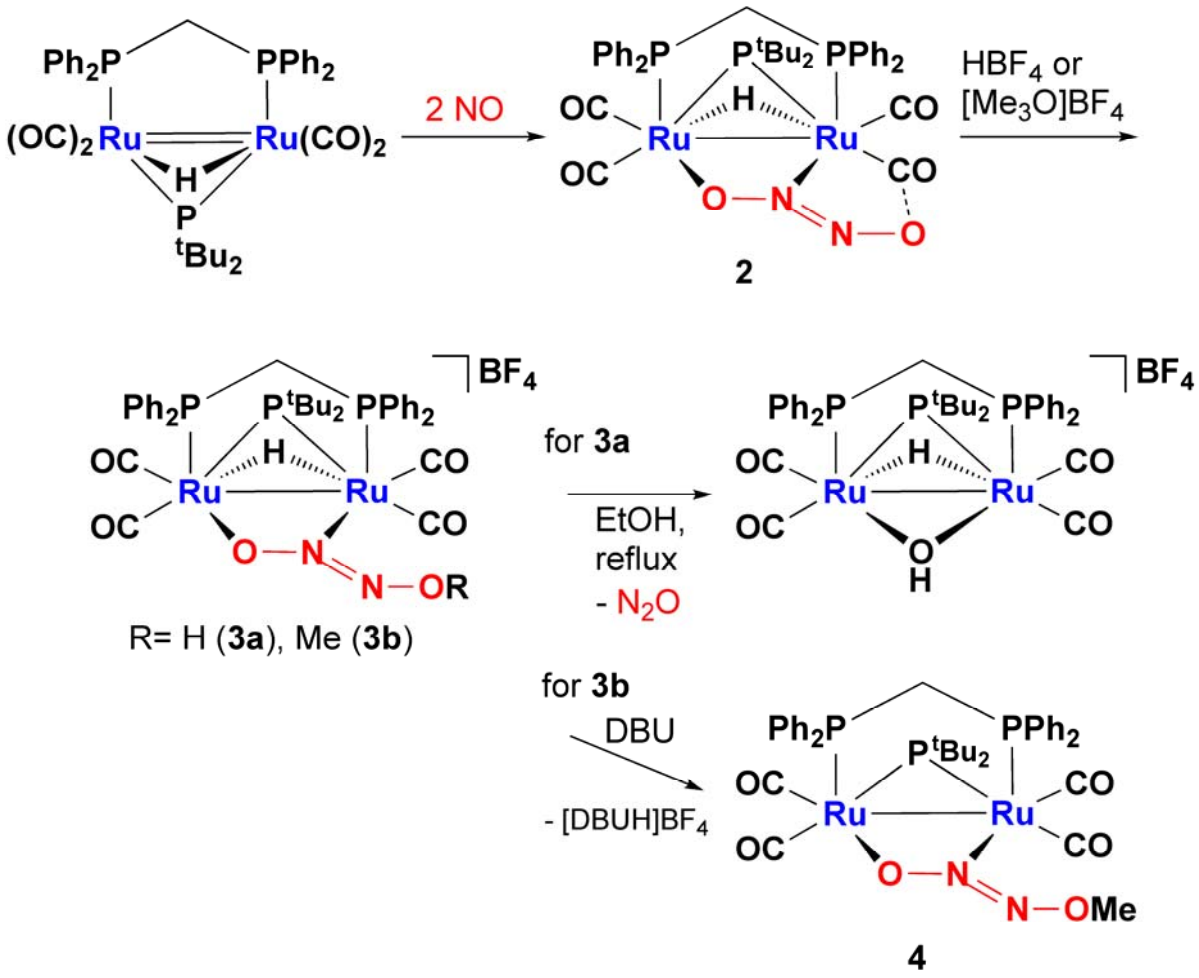

Scheme 2. Synthesis of a *trans*-hyponitrite diruthenium complex **2** and elimination of N_2O.

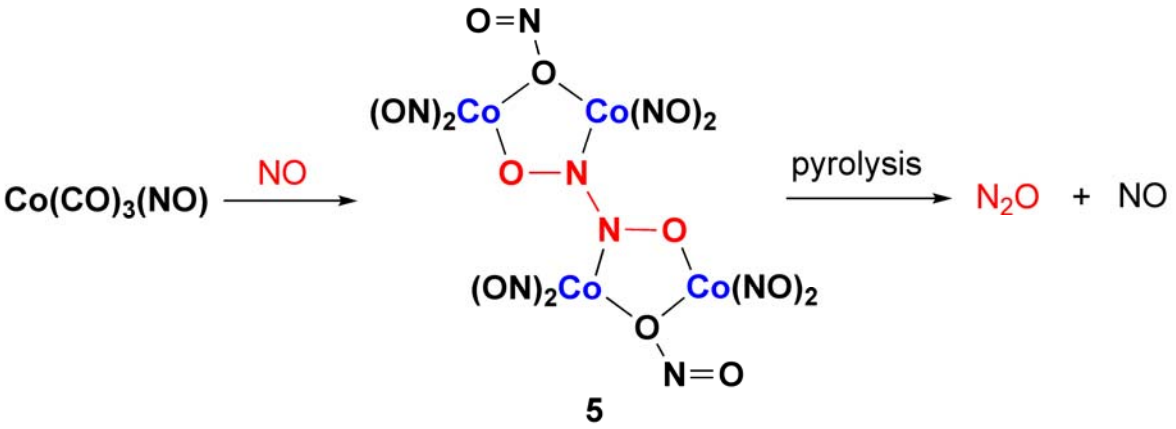

5

Scheme 3. Synthesis of a hyponitrito-bridged cobalt complex **5** and elimination of N_2O.

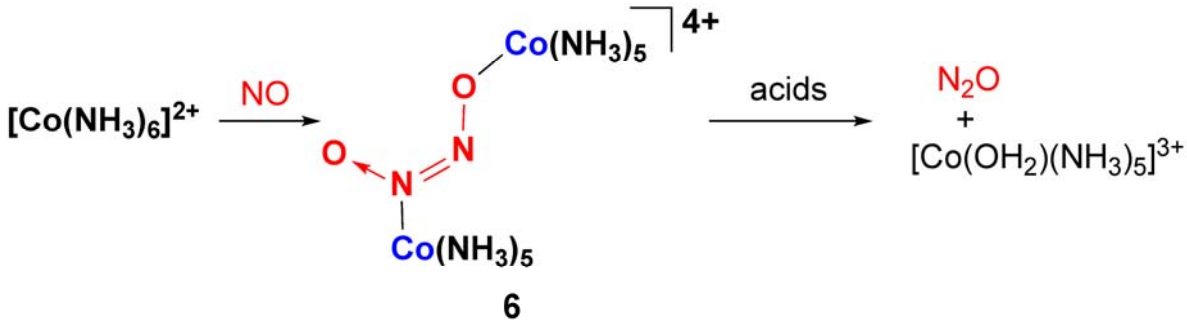

6

Scheme 4. Syntheses of asymmetrical hyponitrito-bridged cobalt complexes **6** and elimination of N_2O.

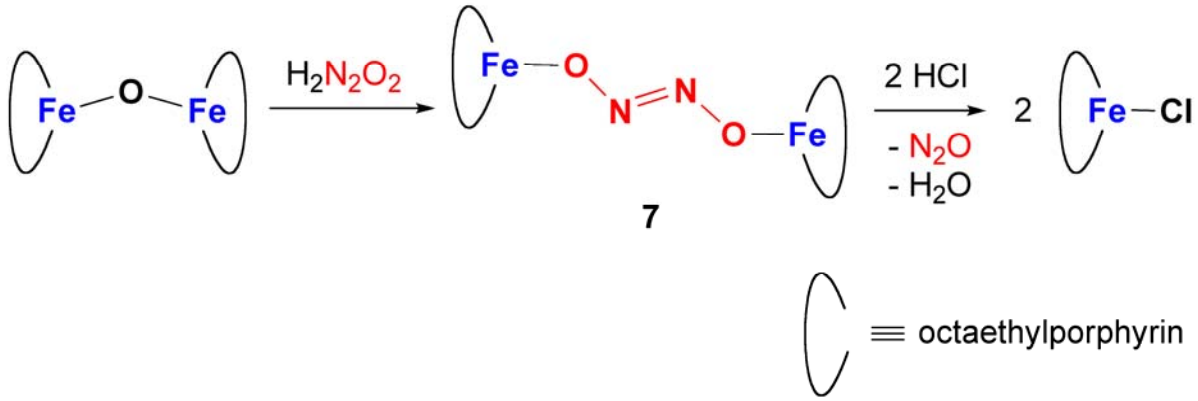

Scheme 5. Synthesis of a hyponitrito-bridged iron porphyrin complex **7** and elimination of N_2O.

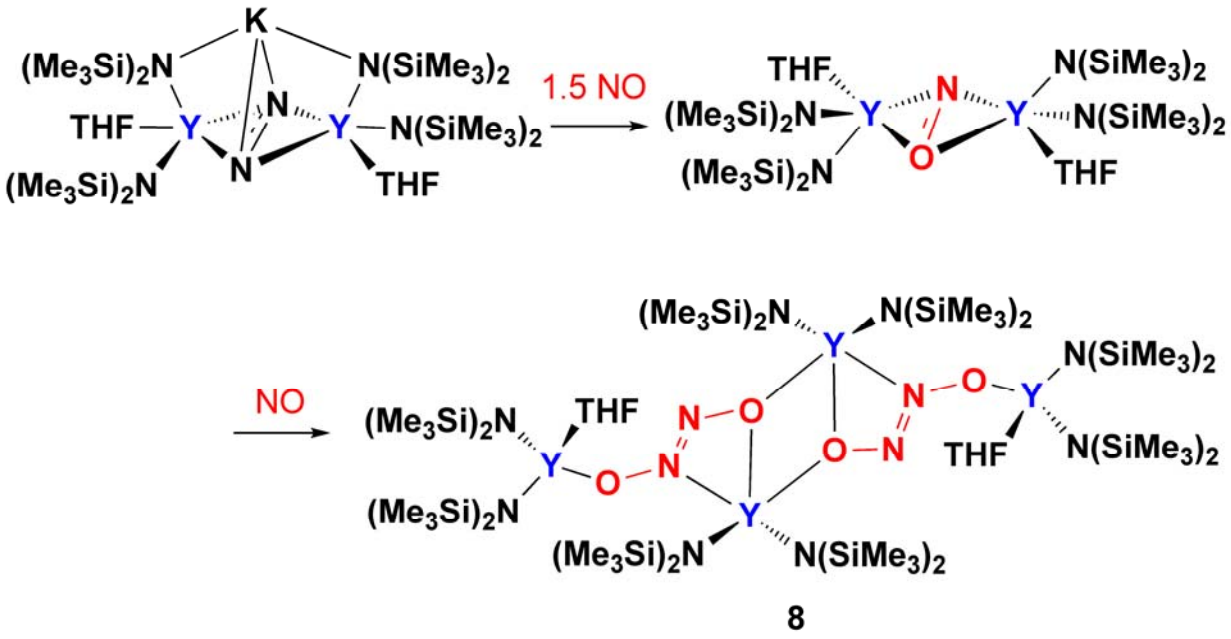

Scheme 6. Synthesis of a *trans*-hyponitrite yttrium complex **8**.

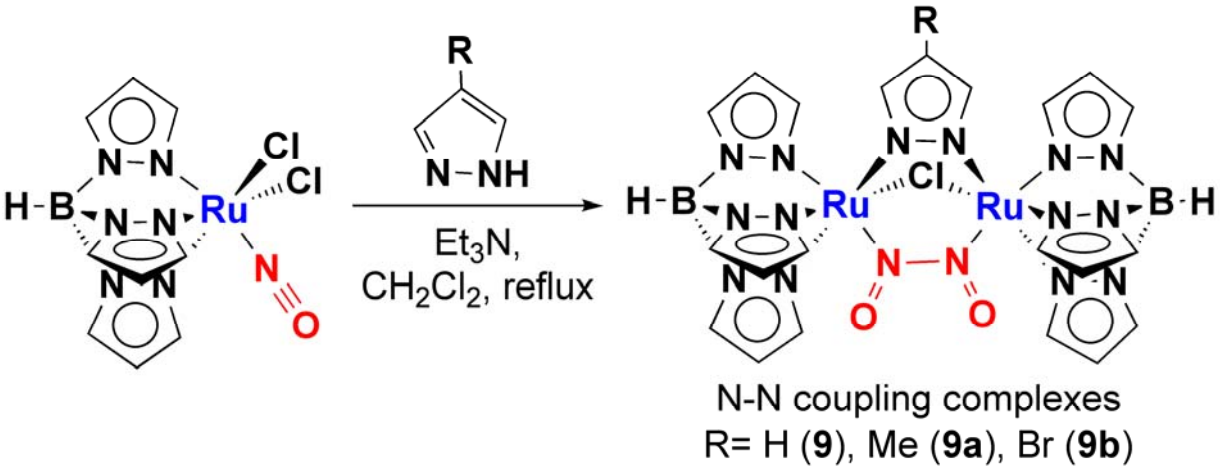

Scheme 7. Syntheses of unusual N–N coupling complexes **9**.

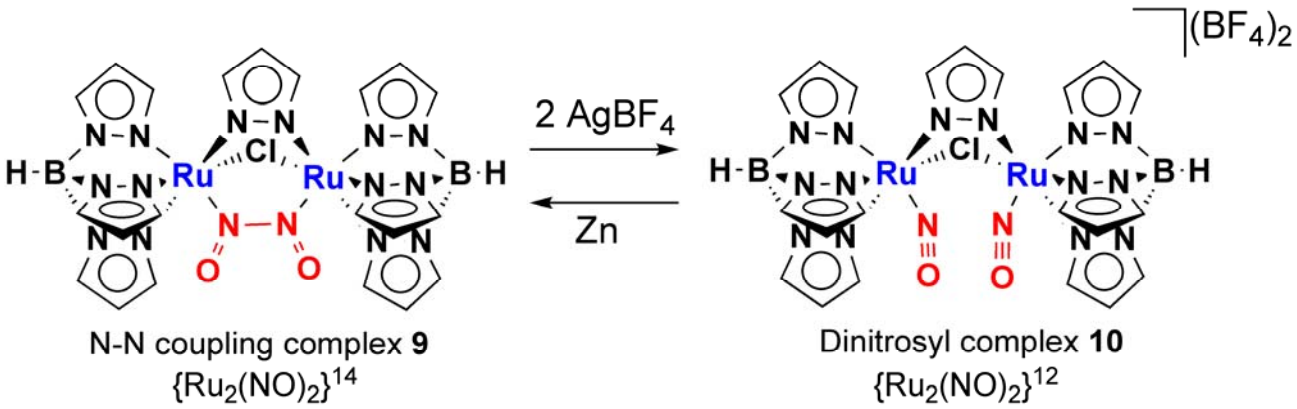

Scheme 8. Redox reactions of an unusual N–N coupling complex **9**.

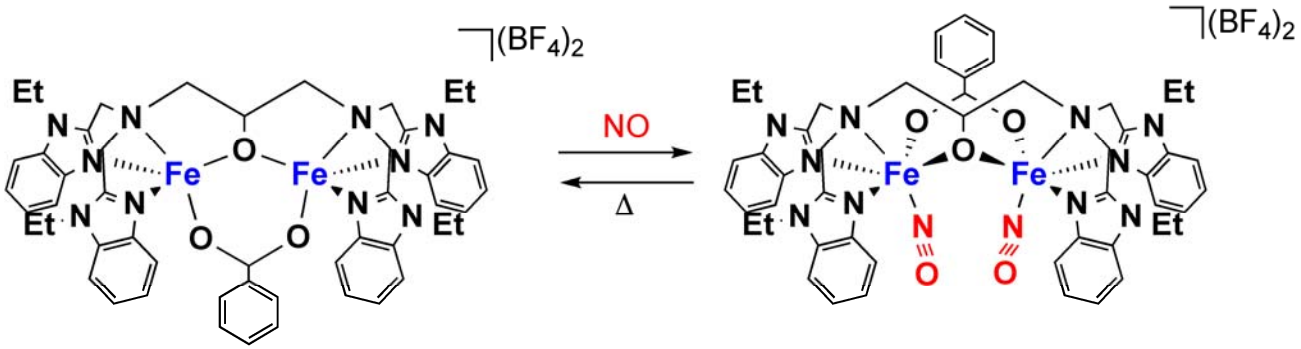

Scheme 9. Attempts to form an N–N bond of two NO ligands on a dinuclear iron complex.

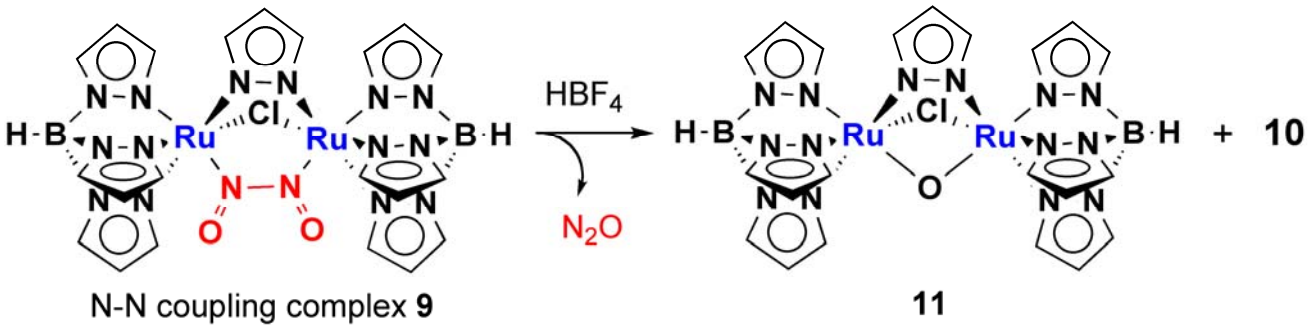

Scheme 10. Elimination of N_2O that is induced by protonation of **9**.

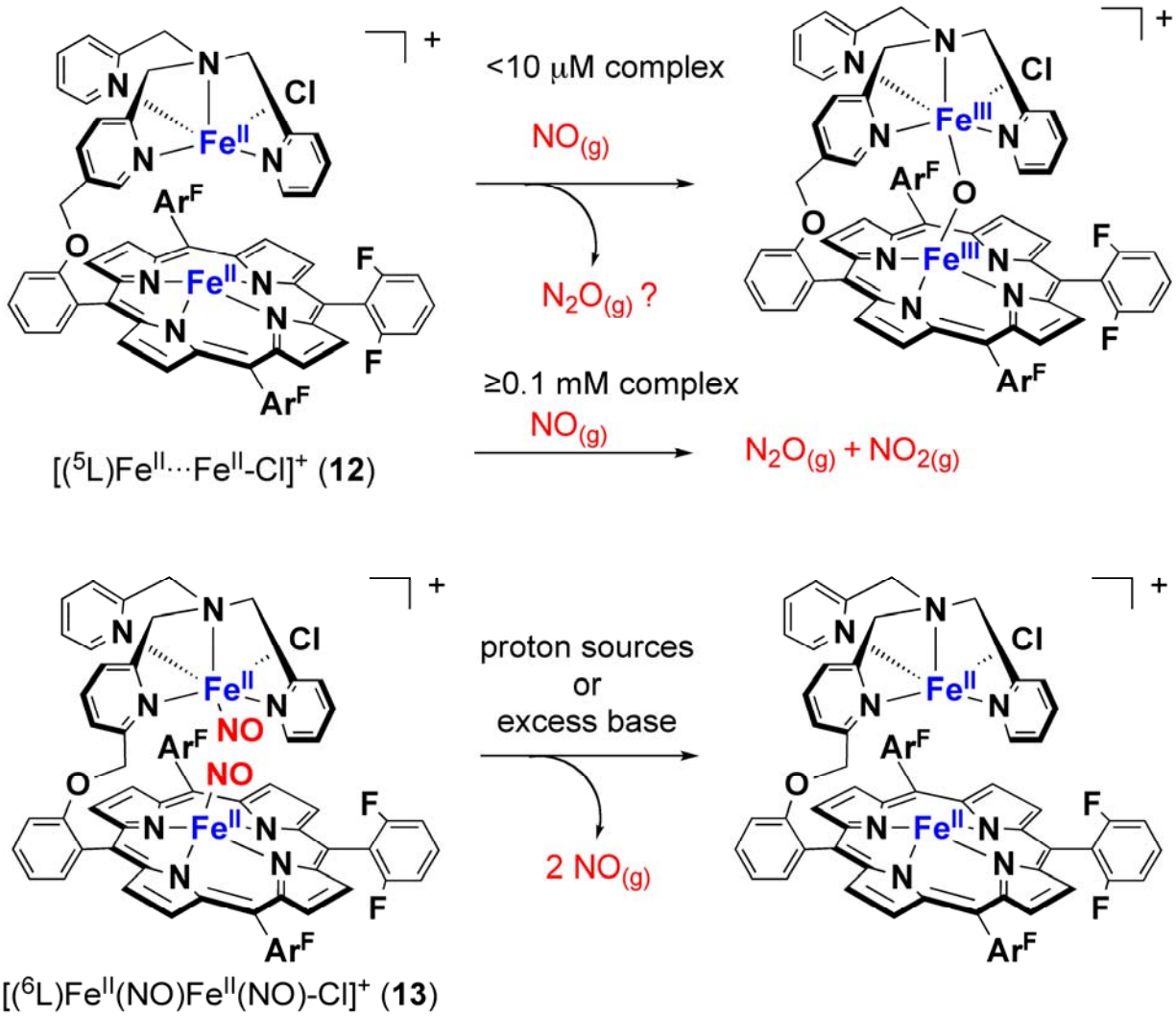

Scheme 11. NOR activity using a heme Fe/tripyridyl Fe dinuclear system.

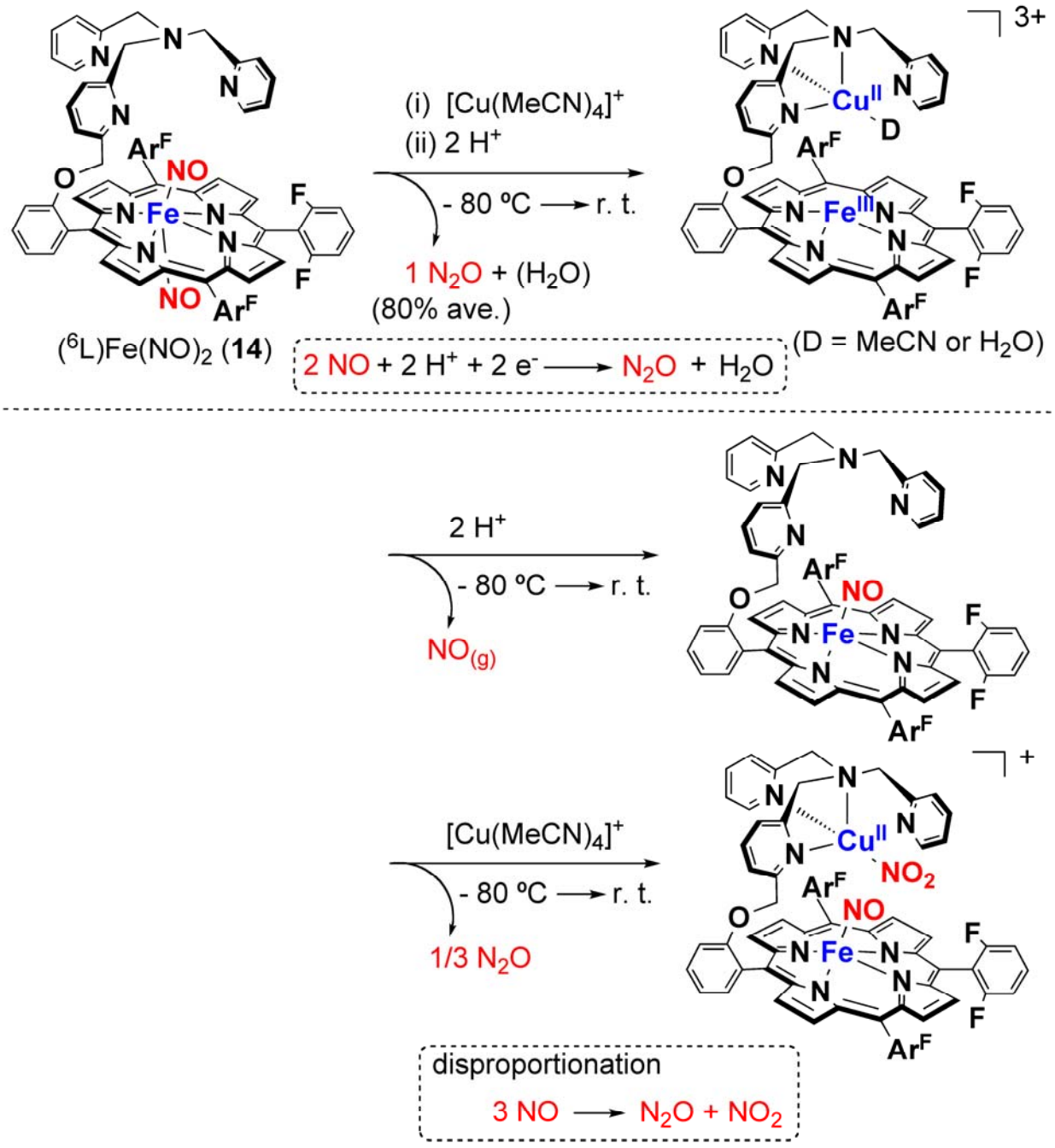

Scheme 12. NOR activity using a heme Fe/tripyridyl Cu dinuclear system.

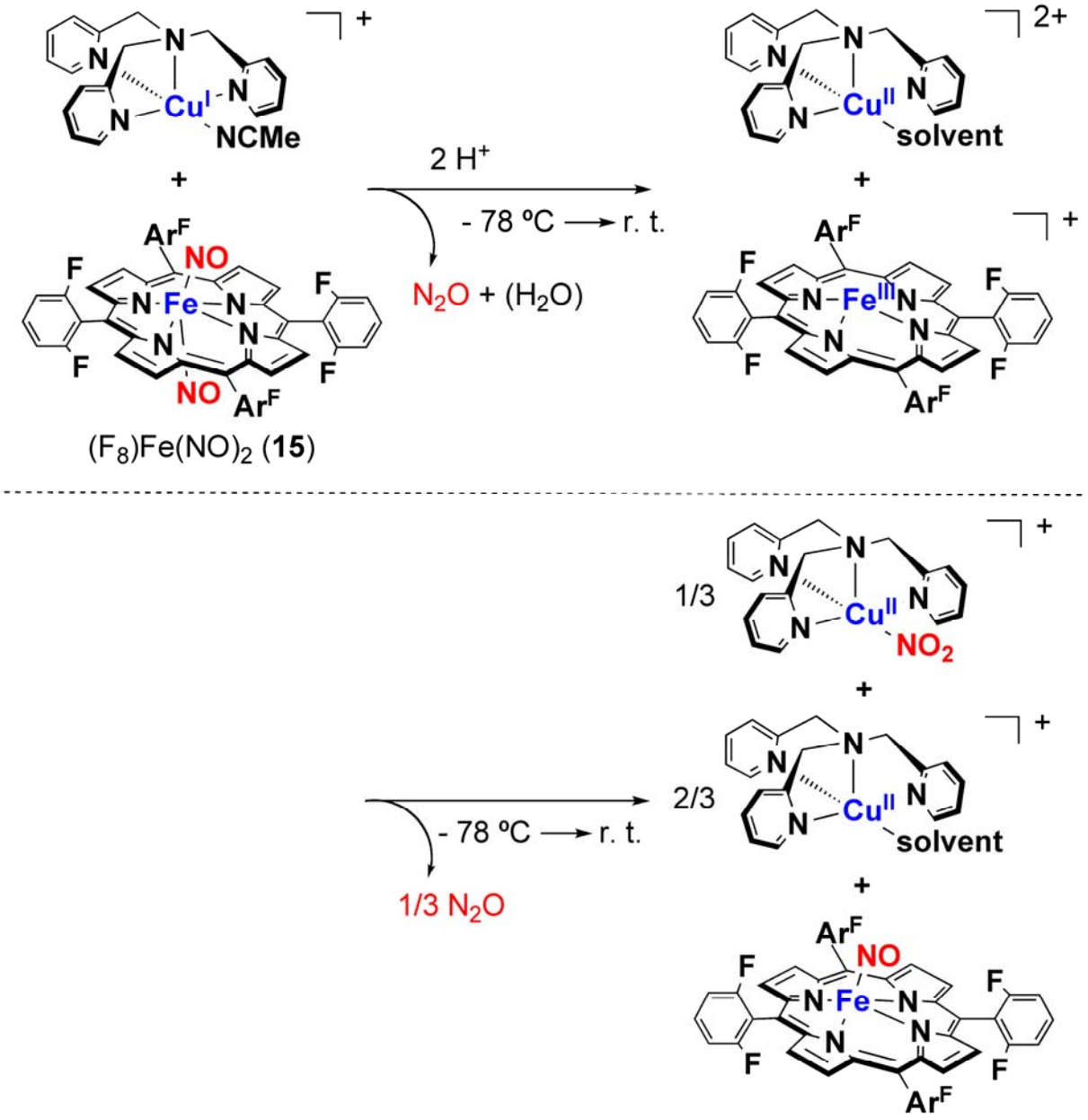

Scheme 13. NOR activity using a 1:1 mixture of a heme Fe and a tripyridyl Cu complex.

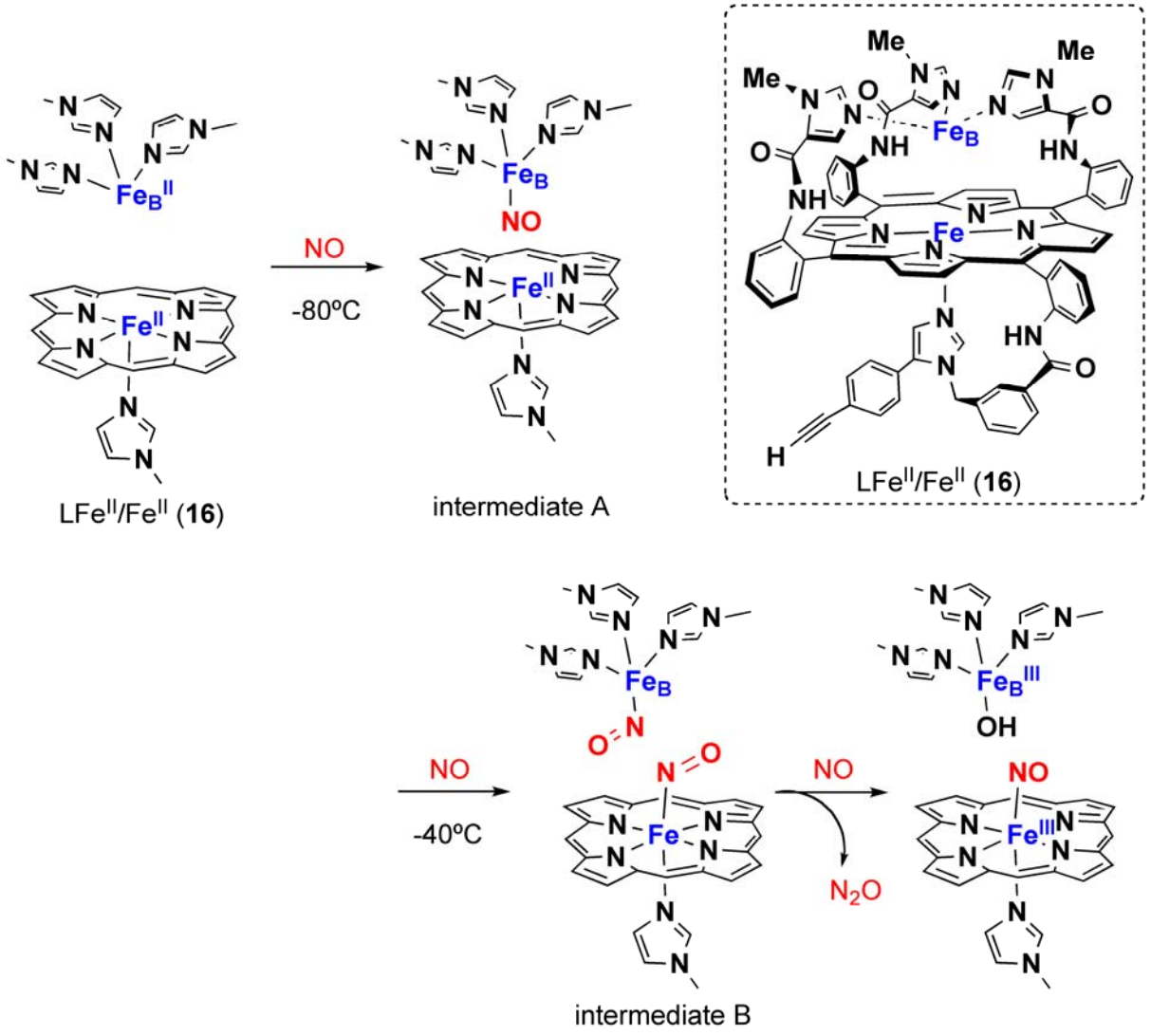

Scheme 14. NOR activity using a heme Fe/trisimidazole Fe dinuclear system.

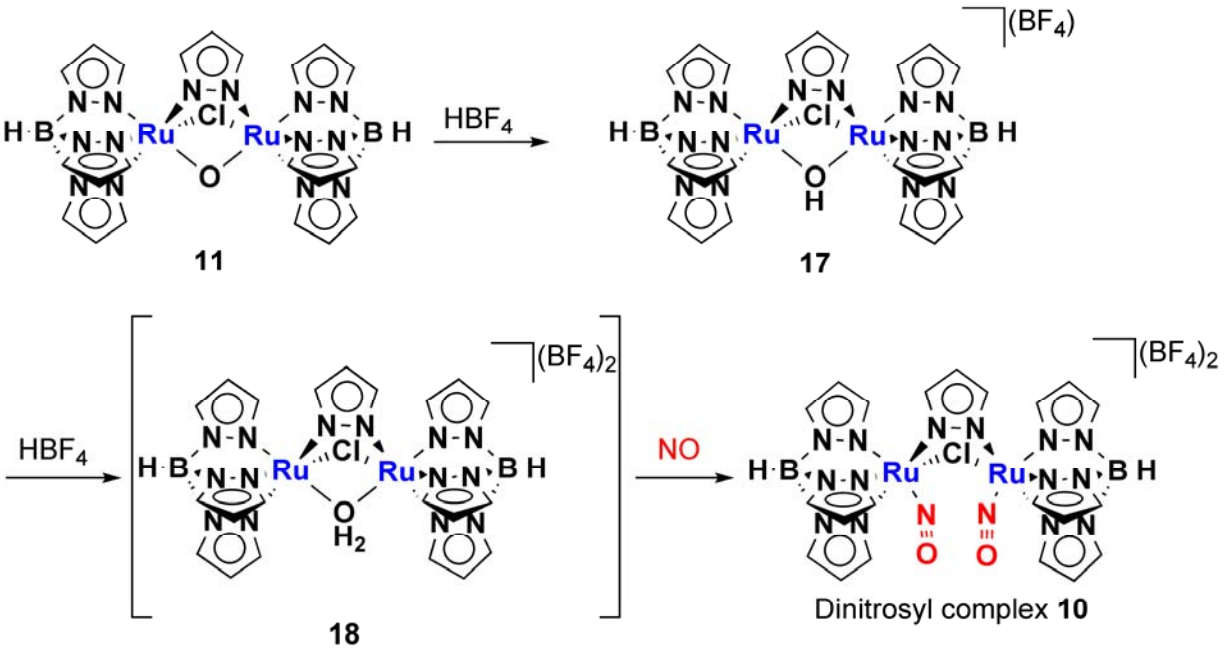

Scheme 15. Double protonation of **11** and subsequent treatment with NO, reforming **10**.

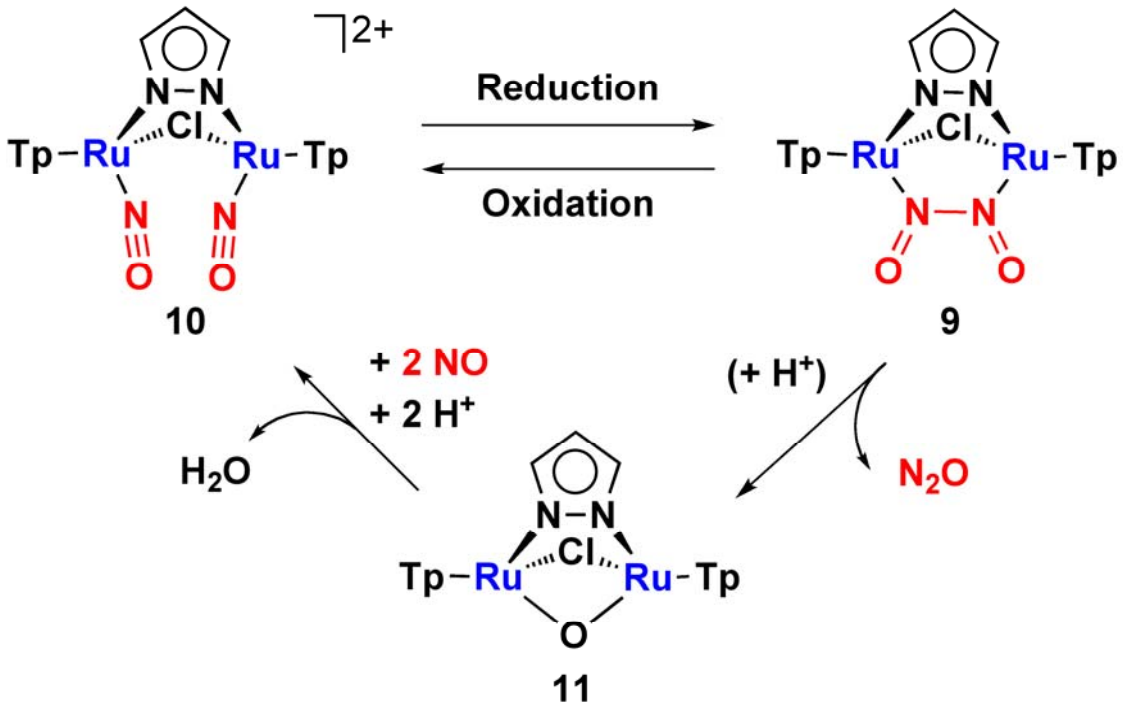

Scheme 16. NO reduction cycle using an unusual N–N coupling complex **9**.

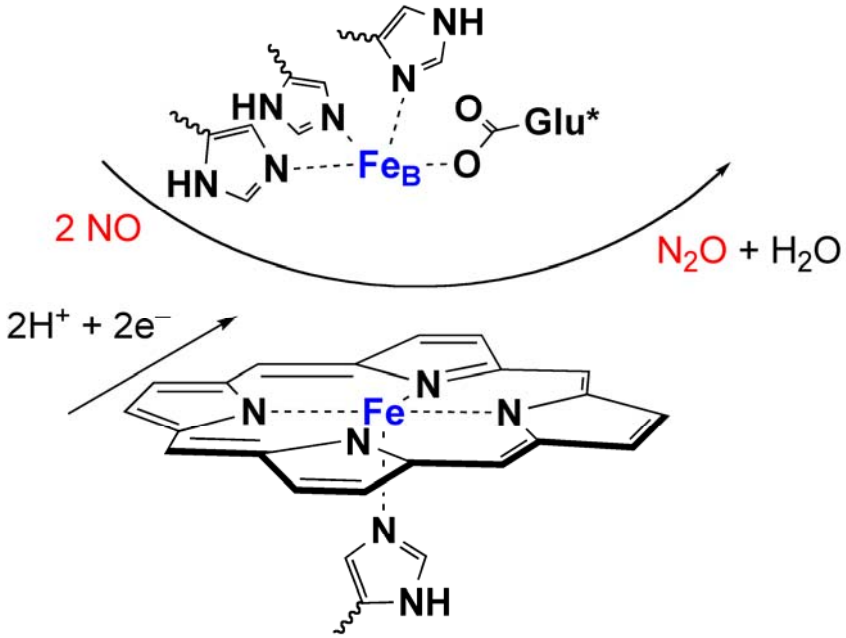

Fig. 1. The active site of nitric oxide reductase (NOR).

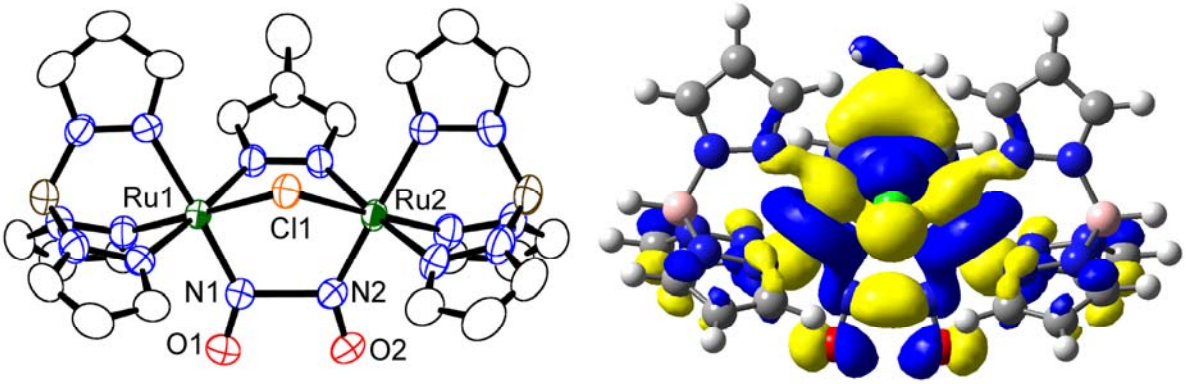

Fig. 2. ORTEP drawing of the molecular structure of **9a** (left) and gaussview depiction of HOMO for the calculated complex **9a** (right).

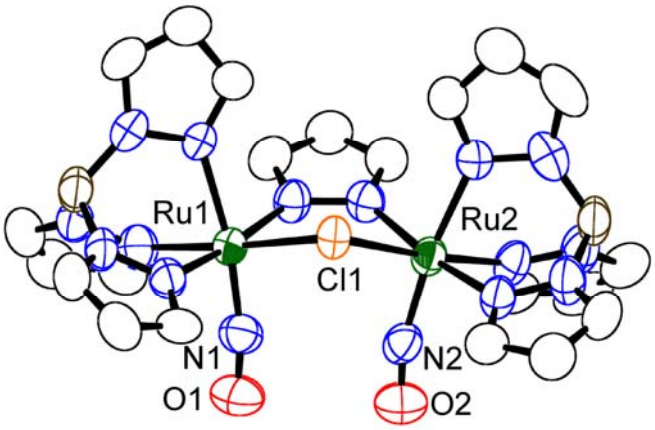

Fig. 3. ORTEP drawing of the molecular structure of **10**. BF_4 counterions are omitted for clarity.

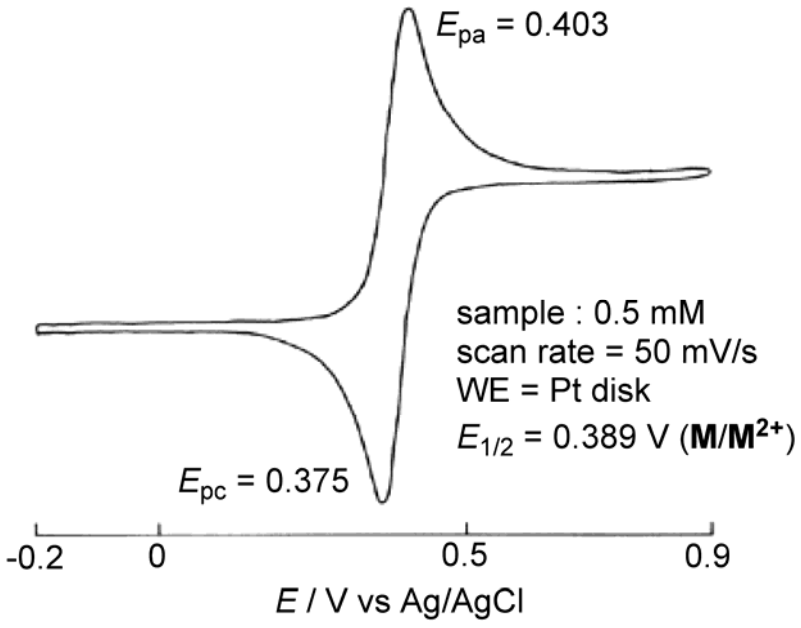

Fig. 4. Cyclic voltammogram of **9** in CH_3CN solution.